Ars Pharmaceutica
https://revistaseug.ugr.es/index.php/ars
E-ISSN: 2340-9894 ISSN: 0004-2927

doi: 10.30827/ars.v67i1.34769
Artículos originales

Multi-Omics and Molecular Dynamics Simulation Reveal the Therapeutic Mechanisms of *Cordyceps sinensis* against Colorectal Cancer

La integración de multi-ómica y la simulación de dinámica molecular revelan los mecanismos terapéuticos de *Cordyceps sinensis* contra el cáncer colorrectal

Xue-mei Zhong[1] 0009-0005-8174-0637
Jia-xin Wen [1]
Peng-fei Wei [1]
[1]Shaoguan University, Medical College, Department of Pharmacy, Shaoguan, China.

Correspondence
Xuemei Zhong
zhongxm7@163.com

Received: 30.08.2025
Accepted: 04.12.2025
Published: 20.12.2025

Funding
This work has been funded by Project the 25th Batch of Education and Teaching Reform Research at Shaoguan University (Grant Number SYJY20241050)

Conflict of interests
The authors declare no conflict of interest.

Resumen

Introducción: El cáncer colorrectal es una neoplasia frecuente. *Cordyceps sinensis*, medicina tradicional china, se ha reportado que tiene potencial terapéutico. Aunque sus compuestos activos y mecanismos moleculares no están del todo esclarecidos. Este estudio tuvo como objetivo explorar los posibles mecanismos frente al cáncer colorrectal mediante farmacología de redes, acoplamiento molecular y dinámica molecular.

Método: Se aplicó un enfoque integrador para identificar compuestos activos y proteínas diana centrales, realizar análisis GO y KEGG, y evaluar las interacciones de unión predichas y la estabilidad del complejo.

Resultados: Se identificaron cinco compuestos principales: ácido araquidónico, cerevisterol, acetato de linoleilo, colesterol y palmitato de colesterol. Las dianas incluyeron SRC, PIK3CA, PIK3CB, PTPN11, JAK2 y PTGS2. Los compuestos mostraron diferentes interacciones de unión predichas con estas dianas, con el colesterol formando el complejo más estable con la proteína central SRC. En contraste, la unión del cerevisterol se asoció con una mayor flexibilidad proteica.

Conclusiones: Los efectos terapéuticos de *Cordyceps sinensis* frente al cáncer colorrectal están mediados por compuestos activos, en especial el colesterol, que forma un complejo estable con SRC. Este estudio proporciona evidencia computacional inicial. El enfoque multi-ómico integrador aporta evidencia sobre sus acciones farmacológicas y resalta su potencial para el desarrollo de nuevos fármacos.

Palabras clave: *Cordyceps sinensis*; Cáncer colorrectal; Farmacología de redes; Acoplamiento molecular; Dinámica molecular

Abstract

Introduction: Colorectal cancer is a prevalent malignancy, and Cordyceps sinensis, a traditional Chinese medicine, is reported to have therapeutic potential. However, the specific active compounds and their underlying molecular mechanisms remain to be fully understood. The objective of this study aimed to explore the potential mechanisms of Cordyceps sinensis against colorectal cancer by combining network pharmacology, molecular docking, and molecular dynamics simulations.

Method: We used an integrative approach of network pharmacology, molecular docking, and molecular dynamics simulations. Through these methods, we identified the major active compounds and their core target proteins, performed GO and KEGG enrichment analyses, and evaluated the predicted binding interactions and complex stability between the active compounds and key targets.

Results: We identified five major active compounds: arachidonic acid, cerevisterol, linoleyl acetate, cholesterol, and cholesteryl palmitate. The core targets of these compounds included SRC, PIK3CA, PIK3CB, PTPN11, JAK2, and PTGS2. The compounds exhibited different predicted binding interactions to these targets, with cholesterol forming the most stable complex to the core target SRC. In contrast, cerevisterol binding was associated with greater protein flexibility.

Conclusions: This study provides initial computational evidence that the therapeutic mechanisms of Cordyceps sinensis against colorectal cancer are mediated by its active compounds, particularly cholesterol, which forms a stable complex with the SRC protein. This integrative multi-omics approach offers valuable scientific evidence for the pharmacological actions of Cordyceps sinensis and underscores its potential for further drug development.

Keywords: *Cordyceps sinensis*; Colorectal cancer; Network pharmacology; Molecular docking; Molecular Dynamics

Highlights

Cordyceps sinensis, a traditional Chinese medicine, shows therapeutic potential against colorectal cancer, but its active compounds and specific molecular mechanisms are not yet fully understood. This study used an integrative approach of network pharmacology, molecular docking, and molecular dynamics to identify potential key compounds and therapeutic mechanisms of *Cordyceps sinensis* against CRC. The findings suggest that *Cordyceps sinensis*, particularly its cholesterol component, may contribute to CRC modulation through stable interactions with core proteins to treat colorectal cancer, providing theoretical insights for future pharmacological exploration.

Introduction

Colorectal cancer (CRC) ranks as the third most prevalent malignancy worldwide and the second leading cause of cancer mortality, with nearly 1.8 million new cases and 881,000 deaths in 2018, and projections of 2.5 million annual cases by 2035[1]. Risk factors include age, genetic predisposition such as Lynch syndrome, chronic inflammation, obesity, physical inactivity, alcohol intake, and diets rich in red or processed meat. CRC is often asymptomatic in early stages, delaying diagnosis and worsening prognosis; screening methods such as colonoscopy improve survival. The 5-year survival rate is about 64% overall but decreases to 12% in metastatic disease, underscoring the need for novel therapeutic strategies[2].

Current treatments include surgery, adjuvant chemotherapy (e.g., 5-fluorouracil and FOLFOX), radiotherapy, and targeted agents such as cetuximab and bevacizumab. Immunotherapy with pembrolizumab has shown benefit in microsatellite-unstable CRC[3]. Complementary approaches, particularly Traditional Chinese Medicine (TCM), are increasingly studied. Tea polyphenols, Ganoderma lucidum, and NSAIDs exhibit anti-CRC effects via antioxidant, anti-inflammatory, and pro-apoptotic mechanisms[4].

Cordyceps sinensis ("Dong Chong Xia Cao"), a medicinal fungus native to the Qinghai-Tibetan Plateau, has long been used in TCM for immune modulation and tumor suppression[5]. Its bioactive components, such as cordycepin and polysaccharides, have been reported to exert cytotoxic, anti-metastatic, and pro-apoptotic effects in CRC, especially when combined with chemotherapy. However, its precise mechanisms remain unclear.

Network pharmacology and molecular dynamics (MD) simulation enable the systematic exploration of multi-component, multi-target characteristics of TCM [6,7]. In this study, these computational approaches were integrated to elucidate the potential therapeutic mechanisms of *Cordyceps sinensis* against CRC.

Methods

Selection of the main active compounds

Compounds of *Cordyceps sinensis* were retrieved from TCMSP[8]. Screening employed OB≥30% and DL≥ 0.18 as conventional criteria, while acknowledging that such thresholds may exclude bioactive compounds with poor predicted pharmacokinetics but relevant local activity. SMILES structures were obtained from PubChem and imported into SwissTarget Prediction to identify potential human targets with probability ≥1%.

Collection of Genetic Targets for Colorectal Cancer

CRC-related target genes were collected from GeneCards, DisGeNET, and OMIM using the Relevance Score[9]. GeneCards searches used "Colorectal Cancer" with Relevance Score >10; duplicates were removed in Excel to generate the final CRC target list.

Research on PPI Networks

A protein-protein interaction (PPI) network was constructed via STRING[10] using "Multiple proteins" and "Homo sapiens," with highest confidence (0.900) and disconnected nodes hidden. The network TSV file was imported into Cytoscape 3.10.2 to calculate topological features including degree, betweenness centrality (BC), and closeness centrality (CC). Nodes meeting intermediate values of degree, BC, and CC were defined as central hubs, representing key targets. The common targets of *Cordyceps sinensis* against CRC were input into DAVID 6.8 for Gene Ontology (GO) and Kyoto Encyclopedia of Genes and Genomes (KEGG) pathway enrichment analysis[11]. Visualization was performed on the Bioinformatics platform using bubble charts based on GeneRatio, Count, and P-values, summarizing enriched biological processes and pathways associated with the target network.

Molecular docking

Molecular docking was performed to predict interactions between *Cordyceps sinensis* active compounds and core CRC targets[12]. PDB files of high-degree protein targets were downloaded from RCSB PDB and processed in PyMOL. Top five active compounds were obtained from PubChem and ChemSpider, converted to PDB via Open Babel. All receptor proteins were treated as rigid, whereas ligands were kept fully flexible during docking. Binding sites were defined based on co-crystal ligand binding and supported by literature reports describing the same active pockets. Proteins and ligands were prepared in AutoDock Tools 1.5.7 and docking executed with AutoGrid/AutoDock. Docking validation was performed by redocking co-crystallized ligands in SRC (PDB: 1US0) and PIK3CA (PDB: 8EXL) using the same parameters as for target docking.The heavy-atom RMSD values were 2.42 Å and 0.98 Å, respectively, indicating good agreement with the experimental poses and confirming the reliability of the docking protocol. Docking energies were used as semi-quantitative indicators of binding tendency (<0 kcal/mol for spontaneous interaction, around −5 kcal/mol for moderate binding, and around −7 kcal/mol for stronger predicted affinity) [13].

Molecular Dynamics Simulation

Molecular dynamics (MD) simulations were performed using GROMACS 2023.2 to assess the stability and interactions of protein–ligand complexes from docking[14]. Protein topology was generated via pdb2gmx with AMBER99SB-ILDN and TIP3P water; ligand topology used sobtop_1.0 with GAFF. The complex was solvated in an octahedral water box, neutralized with counter-ions, and energy-minimized using steepest descent. Equilibration involved NVT and NPT ensembles at 310 K and 1 bar[15]. A 100 ns production run was performed under periodic boundary conditions. Trajectories were analyzed for root mean square deviation (RMSD), root mean square fluctuation (RMSF), radius of gyration (Rg), and hydrogen bonds; plots were visualized using QtGrace. Only cholesterol–SRC and cerevisterol–SRC complexes were simulated, selected as representative top-ranked pairs by docking score (comparative), with each run for 100 ns for qualitative assessment. Each simulation was performed once for a 100 ns trajectory, which provides sufficient sampling for qualitative stability assessment.

Results and Discussion

Key Active Compounds Screening in *Cordyceps sinensis*

Seven principal active compounds in *Cordyceps sinensis* were identified via TCMSP with OB ≥30% and DL ≥0.18, including arachidonic acid, linoleyl acetate, cholesterol, and beta-sitosterol (**Table 1**). Their SMILES were retrieved from PubChem and submitted into SwissTargetPrediction[16], yielding 419 predicted targets, with 282 unique targets after removing duplicates.

Table 1. Active Components of *Cordyceps sinensis*[16]

Mol ID	Molecule name	OB (%)	DL	Numbers of targets
MOL001439	arachidonic acid	45.57	0.20	100
MOL001645	Linoleyl acetate	42.10	0.20	75
MOL000358	beta-sitosterol	36.91	0.75	44
MOL011169	Peroxyergosterol	44.39	0.82	44
MOL008998	cerevisterol	39.52	0.77	100
MOL008999	cholesteryl palmitate	31.05	0.45	51
MOL000953	cholesterol (CLR)	37.87	0.68	56

Overlap of Colorectal Cancer and *Cordyceps sinensis* Targets

Using GeneCards with Relevance Score >10, 2,101 colorectal cancer-related gene targets were identified. These were intersected with 282 predicted targets of *Cordyceps sinensis* bioactive compounds. The analysis revealed 114 overlapping targets (Figure 1), representing key potential therapeutic targets mediating the anti-CRC effects of *Cordyceps sinensis*.

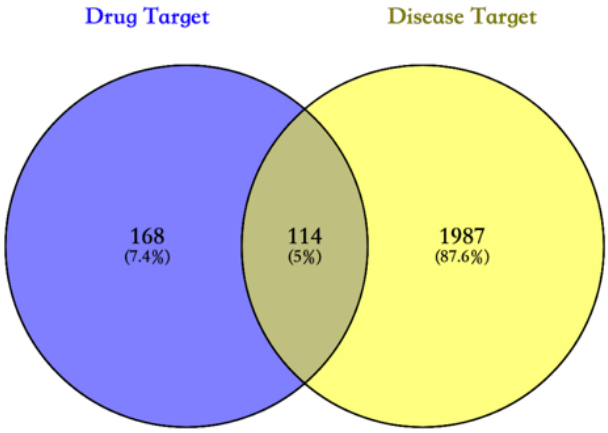

Figure 1. Gene targets represented by Venn diagram

PPI Network Analysis

A PPI network of 114 common targets of *Cordyceps sinensis* against CRC was constructed using STRING and visualized in Cytoscape (**Figure 2a**). The network consisted of 114 nodes connected by 184 edges, with an average node degree of 3.23, local clustering coefficient of 0.504, and PPI enrichment p-value <1.0e-16. Filtering by Betweenness ≥0.123, Closeness ≥0.168, and Degree ≥16 identified five hub targets: SRC, PIK3CA, ESR1, PTGS2, and CYP3A4. Node size and color in **Figures 2b–2c** correspond to Degree values, indicating the topological importance of each protein. SRC exhibited the highest connectivity (Degree = 36), followed by PIK3CA (32), PIK3CB (30), PTPN11 (24), JAK2 (22), PTGS2 (22), ESR1 (20), MAPK8 (20), CYP3A4 (18), and PTGS1 (18). These hub proteins may represent key regulatory nodes within the network and were prioritized for subsequent docking analysis, reflecting potential—but not yet confirmed—therapeutic relevance SRC, a proto-oncogene tyrosine kinase, regulates transcription, immunity, proliferation, apoptosis, motility, and malignant transformation[17], with elevated activity linked to multiple cancers. PIK3CA/PIK3CB activate the PI3K/AKT pathway, controlling proliferation, apoptosis, and migration[18]. PTPN11 influences cell division, DNA repair, metastasis, and angiogenesis[19]. JAK2 mediates hematopoietic signaling[20]. PTGS2, ESR1, and MAPK8 modulate inflammation and tumor progression[21]. Together, these targets outline a predicted multi-target regulatory network of *Cordyceps sinensis* against CRC.

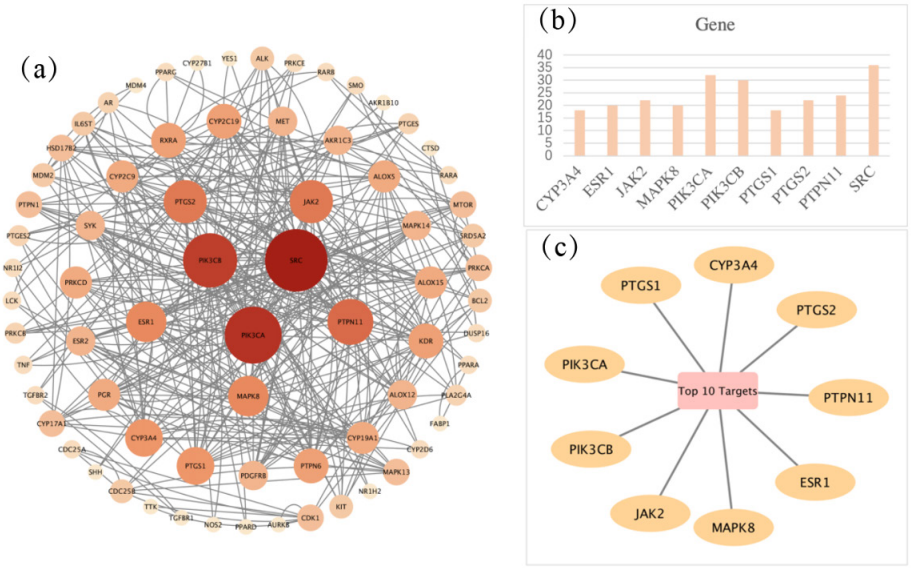

Figure 2.a Identification of core molecular targets. **b** Top-ranked protein targets (n=10) were selected from the PPI network based on degree scores. **c** The interaction network of the 10 highest-ranked targets was visualized using Cytoscape

GO and KEGG Pathway Enrichment Analysis

The 114 common targets of *Cordyceps sinensis* in CRC were analyzed using DAVID 6.8 for GO and KEGG enrichment. GO analysis identified 528 biological process (BP), 135 molecular function (MF), and 45 cellular component (CC) entries; top 20 entries by Count ($P < 0.05$) were selected. KEGG analysis identified 156 pathways, with the top 20 enriched pathways indicating major biological associations. GO enrichment suggested involvement in phosphorylation, signal transduction, transcriptional regulation, and protein modification processes. KEGG pathways included “pathways in cancer”, AGE-RAGE signaling, TRP channels, proteoglycans in cancer, and insulin resistance. A “drug–component–target–pathway” network comprising 133 nodes and 527 edges was constructed to integrate these associations. These enrichments outline the main biological processes potentially involved in the pharmacological effects of *Cordyceps sinensis* against CRC.

Molecular Docking Results

Matching 7 active components of *Cordyceps sinensis* with 114 CRC-related targets revealed that all compounds interact with multiple targets, with arachidonic acid and cerevisterol engaging 42 and 46 targets, respectively. Cytoscape analysis identified five major components by Degree value: arachidonic acid, cerevisterol, Linoleyl acetate, CLR, and cholesteryl palmitate. Molecular docking between the top five compounds and six core targets (SRC, PIK3CA, PIK3CB, PTPN11, JAK2, PTGS2) generated 30 docking results, summarized in Table 2. All ligands displayed negative docking energies, suggesting thermodynamically favorable interactions. CLR and cerevisterol showed the lowest predicted energies with SRC, while CLR also adopted stable binding poses with PIK3CA, JAK2, and PTGS2, reflecting its broad interaction potential. Consistent with these observations, other hub targets such as PIK3CA and PTGS2 also exhibited stable binding with multiple compounds, aligning with their high connectivity in the PPI network. These results suggest that *Cordyceps sinensis* may exert anti-CRC activity through

coordinated modulation of several signaling nodes rather than a single target. Docking results indicate that cholesterol may preferentially interact with SRC, whereas other compounds exhibit broader multi-target associations, supporting a potential synergistic mechanism. Docking scores were used as semi-quantitative indicators of binding tendency and should be interpreted cautiously.

Table 2. Predicted docking energies (kcal/mol) of the compounds with protein targets

Target protein	PDB ID	Docking energy (Kcal/mol)				
		arachidonic acid	cerevisterol	Linoleyl acetate	CLR	cholesteryl palmitate
SRC	1US0	-10.98	-12.44	-9.79	-13.18	-11.97
PIK3CA	8EXL	-5.52	-8.17	-3.88	-8.30	-5.51
PIK3CB	AF	-3.35	-6.27	-2.60	-7.06	-4.85
PTPN11	3B7O	-5.44	-7.84	-2.63	-6.81	-4.90
JAK2	8BXH	-6.05	-8.51	-4.71	-8.53	-5.98
PTGS2	5F19	-4.70	-7.26	-4.92	-8.31	-3.80

Molecular dynamics

MD simulations showed that cholesterol binding to SRC remained relatively stable, enhancing structural compactness, whereas cerevisterol binding was associated with higher flexibility and conformational variation. These results provide qualitative insights into binding-induced structural effects but require further experimental validation. The observed differences likely arise from distinct interaction patterns and binding orientations. The chemical structures of cholesterol and cerevisterol, as well as their binding conformations with SRC, are shown in **Figures 3a** and **3b**.

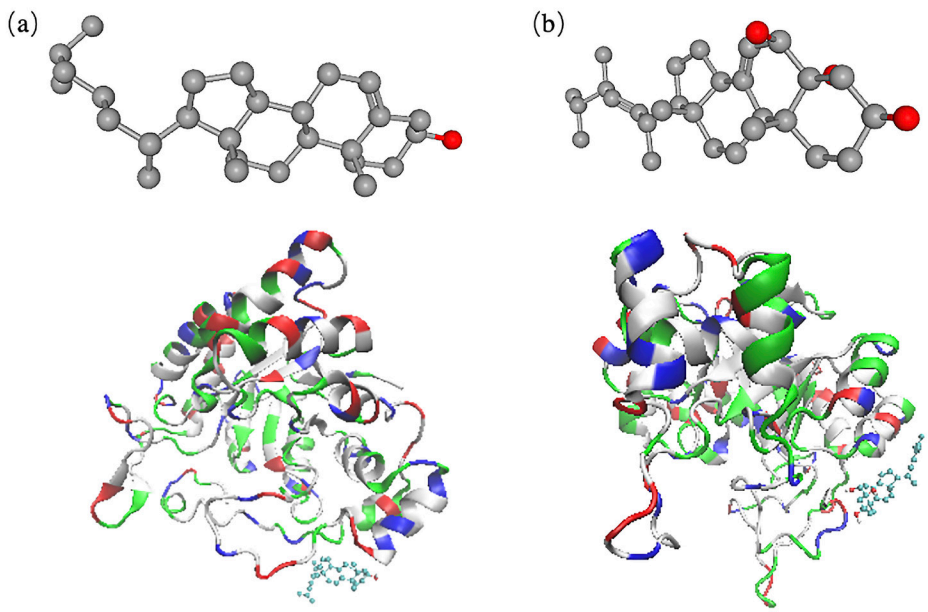

Figure.3a Cholesterol- SRC complex conformer. **b** Cerevisterol- SRC complex conformer

In the 100 ns MD simulation, the RMSD of the Cholesterol-SRC complex remained within 0.10–0.15 nm with a stable trajectory, indicating minimal structural drift. In contrast, the Cerevisterol-SRC complex exhibited higher RMSD values (0.15–0.22 nm) and a pronounced increase between 40–60 ns, indicating lower conformational stability (**Figure 4a**). Rg analysis revealed that both systems maintained overall compactness, but the Cholesterol-SRC complex exhibited a more stable Rg value (1.90–1.95 nm) compared to the slightly higher values of Cerevisterol-SRC (1.95–2.00 nm) (**Figure 4b**). RMSF analysis further supported these findings, as Cholesterol-SRC displayed lower overall fluctuations, whereas Cerevisterol-SRC showed marked flexibility around residue 200 and the C-terminal region (**Figure 4c**). As shown in **Figures 4d**, Solvent Accessible Surface Area (SASA) and hydrogen bond analyses revealed additional differences: the average SASA of Cholesterol-SRC was approximately 145 nm^2, slightly lower than that of Cerevisterol-SRC, suggesting a more compact conformation in solution. Hydrogen bond analysis showed that Cholesterol-SRC formed very few and unstable hydrogen bonds, indicating that its binding was mainly driven by hydrophobic and van der Waals interactions. In contrast, Cerevisterol-SRC was able to maintain 1–3 stable hydrogen bonds after 70 ns (**Figure 5a,5b**), which may contribute to its distinct binding dynamics.

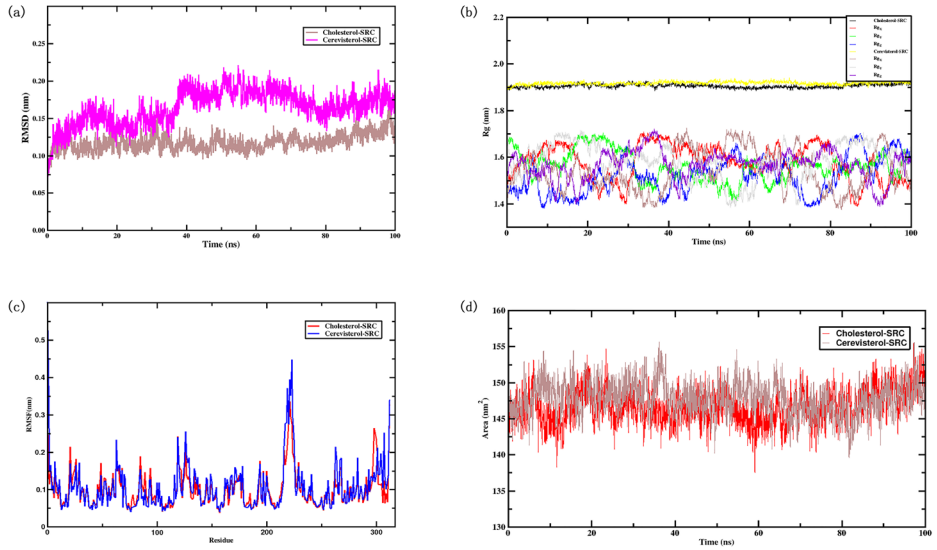

Figure. 4 a RMSD plot of Cholesterol- SRC and Cerevisterol- SRC. **b** Radius of Gyration curve. **c** RMSF curve of Cholesterol- SRC and Cerevisterol- SRC. **d** Solvent Accessible Surface Area (nm^2).

Principal component analysis (PCA) and free energy landscape (FEL) mapping revealed distinct conformational behaviors between the two complexes. The Cholesterol-SRC complex occupied a narrow, well-defined low-energy basin, indicating structural stability with limited conformational diversity. Conversely, the Cerevisterol-SRC complex exhibited multiple, broader basins, suggesting greater conformational flexibility and access to metastable states (**Figures 5c,5d**). Covariance analysis also demonstrated that Cerevisterol-SRC induced strong correlated motions in specific regions, whereas Cholesterol-SRC exhibited relatively weak atomic correlations (**Figure 5e,5f**). Overall, these analyses qualitatively support that cholesterol binding stabilizes the SRC structure, while cerevisterol promotes flexibility and conformational variability, likely due to their different binding modes.

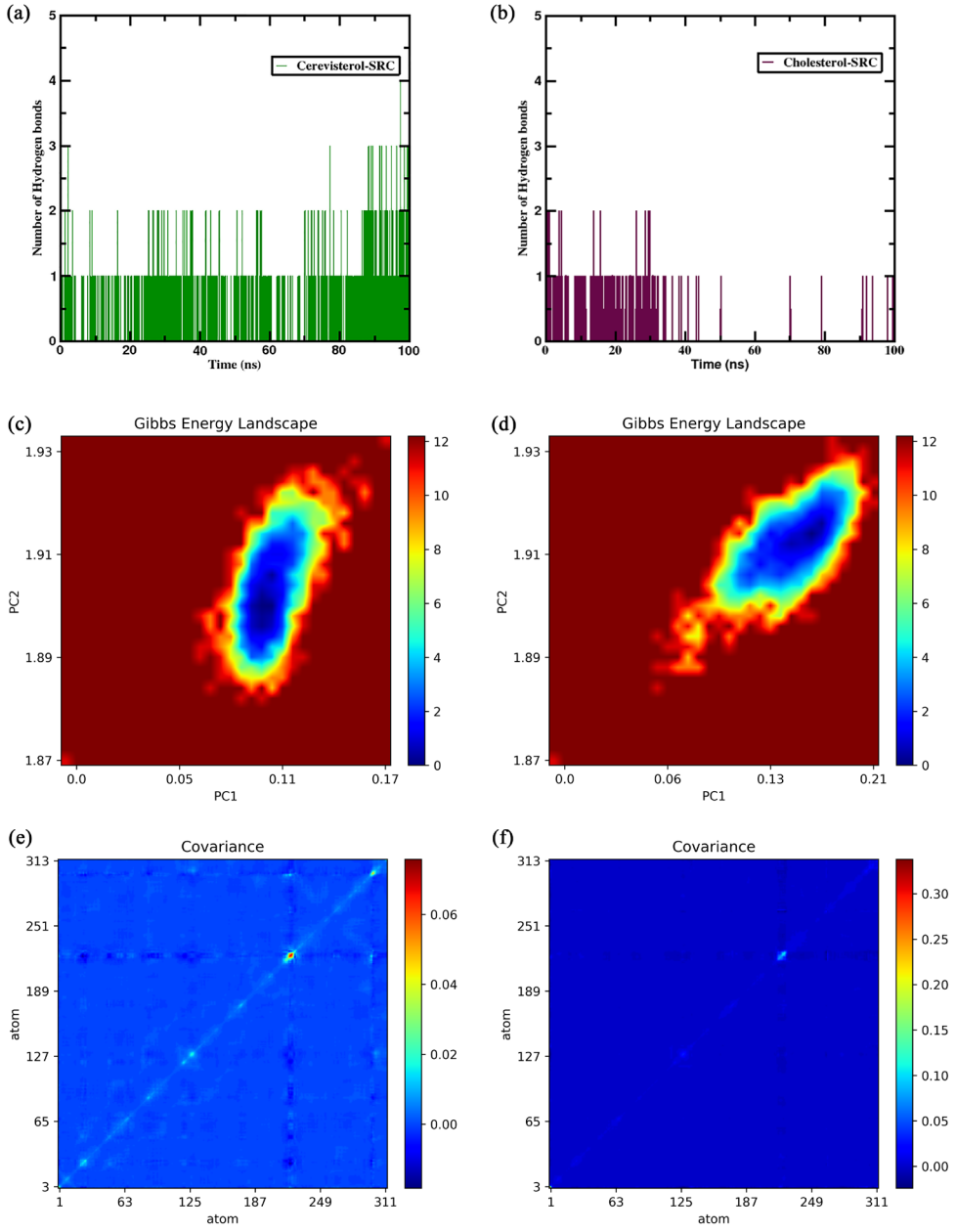

Figure. 5 a the number of hydrogen bonds in the Cholesterol-SRC complex. **b** the number of hydrogen bonds in the Cerevisterol-SRC. **c** Gibbs free energy landscape of the Cholesterol-SRC complex. **d** Gibbs free energy landscape of the Cerevisterol-SRC complex. **e** Covariance matrix of atomic fluctuations for the Cholesterol-SRC complex. **f** Covariance matrix of atomic fluctuations for the Cerevisterol-SRC complex

Conclusions

This study integrated network pharmacology, molecular docking, and molecular dynamics simulations to explore the potential pharmacological mechanisms of *Cordyceps sinensis* against CRC. Key components, including arachidonic acid, cerevisterol, cholesterol, linoleyl acetate, and cholesteryl palmitate, were predicted to interact with core targets such as SRC, PIK3CA, PIK3CB, PTPN11, JAK2, and PTGS2, potentially influencing processes like phosphorylation, signal transduction, and transcriptional regulation through pathways such as oncogenic signaling, AGE-RAGE, TRP channels, and insulin resistance. Molecular dynamics suggested distinct binding behaviors of cholesterol and cerevisterol with SRC, implying possible compound-specific regulatory roles. These findings provide computational insights into the multi-target interactions of *Cordyceps sinensis*, although their biological relevance requires systematic experimental validation.

References

1. Xie YH, Chen YX, Fang JY. Comprehensive review of targeted therapy for colorectal cancer. Signal Transduct Target Ther. 2020;5(1):22. doi:10.1038/s41392-020-0116-z.

2. Benson A. Epidemiology, disease progression, and economic burden of colorectal cancer. J Manag Care Pharm. 2007;13(6 Suppl C):5-18. doi:10.18553/jmcp.2007.13.s6-c.5

3. Ganesh K, Stadler ZK, Cercek A, Mendelsohn RB, Shia J, Segal NH, et al. Immunotherapy in colorectal cancer: rationale, challenges and potential. Nat Rev Gastroenterol Hepatol. 2019;16(6):361-375. doi:10.1038/s41575-019-0126-x.

4. Wang X, Liu Y, Wu Z, Zhang P, Zhang X. Tea polyphenols: a natural antioxidant regulates gut flora to protect the intestinal mucosa and prevent chronic diseases. Antioxidants (Basel). 2022;11(2):253. doi:10.3390/antiox11020253

5. Qi W, Zhou X, Wang J, Zhang K, Zhou Y, Chen S, et al. *Cordyceps sinensis* polysaccharide inhibits colon cancer cells growth by inducing apoptosis and autophagy flux blockage via mTOR signaling. Carbohydr Polym. 2020;237:116113. doi:10.1016/j.carbpol.2020.116113

6. Ma H, Wang G, Guo X, Yao Y, Li C, Li X, et al. Network pharmacology and molecular docking analysis explores the mechanisms of *Cordyceps sinensis* in the treatment of oral lichen planus. J Oncol. 2022;2022:3156785. doi:10.1155/2022/3156785

7. Hansson T, Oostenbrink C, van Gunsteren W. Molecular dynamics simulations. Curr Opin Struct Biol. 2002;12(2):190-196. doi:10.1016/S0959-440X(02)00308-1

8. Ru J, Li P, Wang J, Zhou W, Li B, Huang C, et al. TCMSP: a database of systems pharmacology for drug discovery from herbal medicines. J Cheminform. 2014;6:1-6. doi:10.1186/1758-2946-6-13

9. Stelzer G, Rosen N, Plaschkes I, Zimmerman S, Twik M, Fishilevich S, et al. The GeneCards suite: from gene data mining to disease genome sequence analyses. Curr Protoc Bioinformatics. 2016;54(1):1.30.31–1.30.33. doi:10.1002/cpbi.5

10. Szklarczyk D, Gable AL, Nastou KC, Lyon D, Kirsch R, Pyysalo S, et al. The STRING database in 2021: customizable protein–protein networks, and functional characterization of user-uploaded gene/measurement sets. Nucleic Acids Res. 2021;49(D1):D605-D612. doi:10.1093/nar/gkaa1074

11. Kanehisa M, Goto S. KEGG: kyoto encyclopedia of genes and genomes. Nucleic Acids Res. 2000;28(1):27-30. doi:10.1093/nar/28.1.27

12. Pagadala NS, Syed K, Tuszynski J. Software for molecular docking: a review. Biophys Rev. 2017;9:91-102. doi:10.1007/s12551-016-0247-1

13. Hsin KY, Ghosh S, Kitano H. Combining machine learning systems and multiple docking simulation packages to improve docking prediction reliability for network pharmacology. PLoS One. 2013;8(12):e83922. doi:10.1371/journal.pone.0083922

14. Abraham M, Alekseenko A, Bergh C, Blau C, Briand E, Doijade M, et al. GROMACS 2023.2 manual. Geneva: CERN European Organization for Nuclear Research; 2023. Zenodo.

15. Mundy CJ, Siepmann JI, Klein ML. Decane under shear: a molecular dynamics study using reversible NVT-SLLOD and NPT-SLLOD algorithms. J Chem Phys. 1995;103(23):10192-10200. doi:10.1063/1.469922

16. Ma H, Wang G, Guo X, Li J, Zhang Y, Liu H, et al. Network Pharmacology and Molecular Docking Analysis Explores the Mechanisms of *Cordyceps sinensis* in the Treatment of Oral Lichen Planus. J Oncol. 2022;2022:3156785. doi:10.1155/2022/3156785.

17. Wang N, Liang H, Zhou Y, Wang C, Zhang S, Pan Y, et al. miR-203 suppresses the proliferation and migration and promotes the apoptosis of lung cancer cells by targeting SRC. PLoS One. 2014;9(8):e105570. doi:10.1371/journal.pone.0105570

18. Lino M, Merlo A. PI3Kinase signaling in glioblastoma. J Neurooncol. 2011;103:417-427. doi:10.1007/s11060-010-0442-z

19. Cao Y, Duan H, Su A, Xu L, Lai B. A pan-cancer analysis confirms PTPN11's potential as a prognostic and immunological biomarker. Aging (Albany NY). 2022;14(13):5590. doi:10.18632/aging.204171

20. Freitas RM, Santos MO, Maranduba CMC. The JAK2 gene as a protagonist in chronic myeloproliferative neoplasms. Rev Bras Hematol Hemoter. 2013;35(4):278-279. doi:10.5581/1516-8484.20130074

21. Bai Y, Wang G, Lan J, Wu P, Liang G, Huang J, et al. Mass spectrometric behavior and molecular mechanisms of fermented deoxyanthocyanidins to alleviate ulcerative colitis based on network pharmacology. Int J Anal Chem. 2022;2022:9293208. doi:10.1155/2022/9293208